

## Chapter 5: Moving Together

Some of the most mesmerizing examples of collective behaviour are seen overhead every day. V-shaped formations of migrating geese, starlings dancing in the evening sky and hungry seagulls swarming over a fish market, are just some of the wide variety of shapes formed by bird flocks. Fish schools also come in many different shapes and sizes: stationary swarms; predator avoiding vacuoles and flash expansions; hourglasses and vortices; highly aligned cruising parabolas, herds and balls. These dynamic spatial patterns often provide the examples that first come into our heads when we think of animal groups.

While the preceding three chapters described the dynamics of animal groups, they did not explicitly describe the spatial patterns generated by these groups. For example, the decision-making of insects and fish was studied in situations where individuals have only two or a small number of alternative sites to choose between. In models of these phenomena, space is represented as the number of individuals who have taken each of these alternatives. This approach often simplifies our understanding of the underlying dynamics of these groups, but in doing so it can fail to capture the spatial structure that characterizes them. As a simple consequence of the fact these groups move, we need to give careful consideration to how they change position in space as well as time.

The main tool I will use in describing the dynamics of flocking are self-propelled particle (SPP) models (Czirok & Vicsek 2000; Okubo 1986; Vicsek et al. 1995). In SPP models 'particles' move in a one, two or three dimensional space. Each particle has a local interaction zone within which they respond to other particles. The exact form of this interaction varies between models but typically, individuals are repulsed by, attracted to, and/or aligned with other individuals within one or more different zones. These models allow us to investigate the conditions under which collective patterns are produced by spatially local interactions.

### 5.1 Attraction

Before animals can create spatial patterns they must first come together. In chapter 2, I discussed how and why animal groups form without specific reference to spatial structure. A good starting point for explicitly representing space comes from Niwa (2004). His model, which is an extension of a non-spatial model described in chapter 2, describes groups of individuals that are constrained to move on a lattice (see Box 5.A). Each group performs a random walk and when groups meet they merge. Groups split with a fixed probability per time step. Figure 5.1a shows an example of how composition of these groups changes through time and space. Over time groups 'clump' together. Sites containing large groups are usually located near to other sites containing large

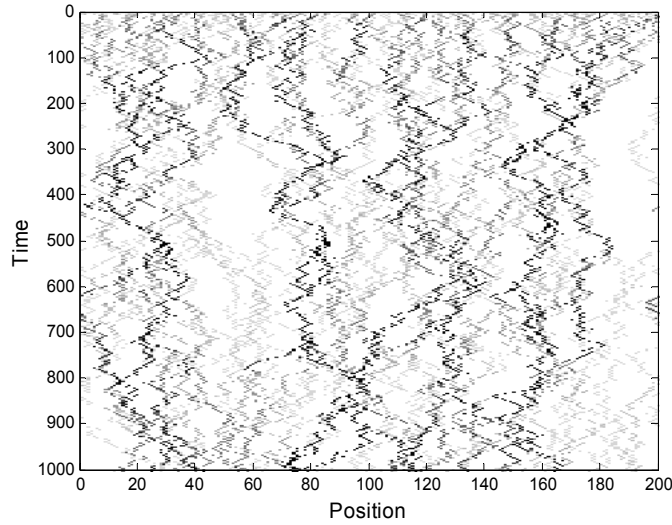
groups, while sites with few individuals are surrounded by other sites with few individuals. The position of these clumps changes through time as the groups move according to a random walk.

### **Box 5.A Niwa's spatial merge and split model**

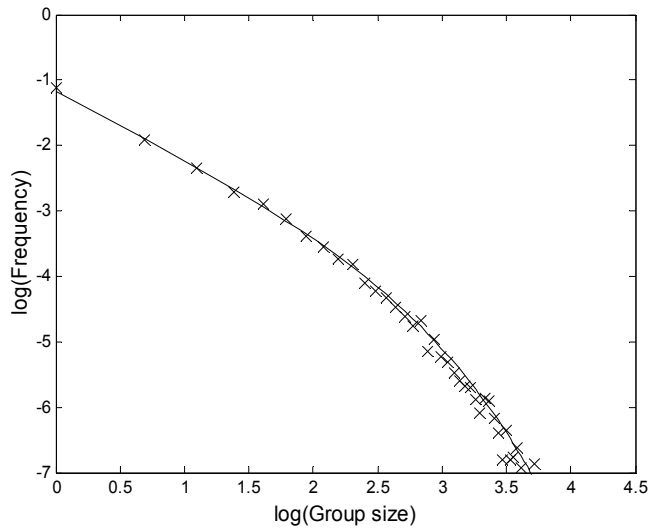
The basic assumptions of this model are the same as in box 2.B. A total of  $m$  individuals are initially randomly distributed across  $s$  sites and  $n_i$  represents the number of individuals on site  $i$ . The key difference in the spatial model is how the groups move. Here we assume that groups move on a  $d$  dimensional lattice of discrete sites, such that each site has  $2d$  neighbouring sites, e.g. in one dimension each site has neighbours to the left and right and in two dimensions each site has neighbours to the north, east, south and west. The lattice is structured so that individuals moving off, for example, the north edge of the lattice reappear at the south. Thus the lattice is a circle in one dimension and a torus in two dimensions. On each time step, each group either moves to one of neighboring sites, each chosen with equal probability  $1/2d$ , or with probability  $p$  the group splits in to two groups, one which stays on the same site and the other which moves to a randomly chosen neighbouring site. When a group splits the size of the two components is chosen uniformly at random, so that all group sizes are equally likely. If two groups of size  $n_i$  and  $n_j$  meet at site  $k$  then they form a new group  $n_k = n_i + n_j$ , thus groups always merge when they meet. The same rule applies if three or more groups meet.

Figure 5.1a shows a simulation of the above model in one dimension ( $d=1$ ). From an initial distribution where each individual occupies one site, larger groups quickly form. These groups perform a random walk and increase in size as they meet other groups. After 1000 time steps there are around five or six large groups and a number of smaller groups. Figure 1b shows the distribution of group sizes at a randomly chosen site over 100,000 time steps of the simulation. Niwa (2004) went on to show that the distribution of group sizes in these simulations is characterized by exactly the same curve as in his earlier non-spatial model (Box 2.B). By finding the mean group size experienced by an individual it is possible to give an expression for the entire distribution of group sizes.

(a)



(b)



**Figure 5.1: Simulation of Niwa's spatial merge and split model.** Simulation of model described in box 5.A with  $s=m=200$  sites/individuals and split probability  $p=0.05$ . Initially each site contains a single individual, i.e. a group of size 1. (a) The time evolution of the number of individuals across the sites. Darker shading indicates larger groups at a particular site, white indicates sites containing no individuals. (b) Shows the distribution of the number of individuals in a randomly chosen site over 100,000 simulation time steps. The solid line is equation 2.1 with  $\langle N \rangle_p$  estimated directly from the simulation.

The unit of description in Niwa's model is the group. The model defines rules for how groups merge and split. The strength of this approach is that it reproduces the empirical distribution of fish school sizes (compare figure 5.1b and figure 2.6). The main limitation of this model is that it does not describe how between-individual interactions produce group dynamics. Establishing such a connection is often the central question in the study of flocking. It is here that self-propelled particle models play an important role.

In the simplest SPP model the only interaction between individual 'particles' is attraction (Box 5.B). Figure 5.2a shows the outcome of a one dimensional SPP model in which individuals are attracted to other individuals within a fixed distance. As in Niwa's model, relatively stable clusters of individuals quickly form. Unlike Niwa's model, larger clusters move slower than solitary individuals. This is because individuals on the edge of the cluster are attracted inwards, resulting in a constant pull towards the centre of the cluster's mass. As clusters increase in size they move less and less, while solitary individuals and smaller groups move and eventually join the clusters (Okubo 1986). After some time a small number of large stationary clusters form.

## Box 5.B Self-propelled particle models

The term self-propelled particle (SPP) was introduced by Vicsek et al. (1995), but the idea of building models where individuals interact through zones of repulsion, attraction and alignment had been proposed independently by a number of authors (Aoki 1982; Gueron et al. 1996; Helbing & Molnar 1995; Okubo 1986; Reynolds 1987). This box presents some of the simplest of these models, including a model of aggregation and Vicsek and co-workers original SPP model of alignment, as well as a more detailed model by Couzin et al. (2002) including repulsion, attraction and alignment.

The general SPP model involves a group of  $N$  particles in a  $d$  dimensional space. Let the vectors  $\underline{x}_i$  and  $\underline{u}_i$  represent the position and velocity individual  $i$ . Let  $r$  represent the interaction radius of the individuals. On each time step  $t$ , all individuals update their position and velocity as follows

$$\begin{aligned}\underline{x}_i(t+1) &= \underline{x}_i(t) + v_0 \underline{u}_i(t+1) \\ \underline{u}_i(t+1) &= \alpha \underline{u}_i(t) + (1-\alpha) \underline{s} + \underline{e}\end{aligned}$$

where  $v_0$  is a constant determining a baseline distance which individuals move per time step and  $\alpha$  is the inertia of an individual (i.e. its tendency to keep the same direction as on the previous time step). The vectors  $\underline{s}$  and  $\underline{e}$  are determined on each time step for each individual.  $\underline{s}$  is a vector (usually a unit vector) with a direction that depends on the position and velocity of the set of particles,  $R_i$ , which are within distance  $r$  of individual, excluding itself.  $\underline{e}$  is a random vector incorporating noise in to the movement of the individual and may also be a function of the position and velocity of  $i$ 's neighbours.

**Attraction:** To model individuals which are attracted to one another the vector  $\underline{s}$  should point towards the average position of an individual's neighbours. In one dimension we can set

$$s = \frac{1}{|R_i|} \sum_{j \in R_i} \text{sign}\{x_j(t) - x_i(t)\}$$

The function  $\text{sign}\{a\}$  returns 1 if  $a > 0$ , -1 if  $a < 0$ , and 0 if  $a = 0$ . We set  $e$  to be a random number selected uniformly at random from a range  $[-\eta/2, \eta/2]$ , where  $\eta$  is a constant.

Figure 5.2a shows a simulation of this model on a one dimensional ring. In this model aggregations form and these move more slowly as their size increases.

**Alignment:** Individuals align by adopting the same direction as their neighbours. In one dimension, Czirok et al. (1999) use

$$s = G\left(\frac{1}{|R_i|} \sum_{j \in R_i} u_j(t)\right) \text{ where } G(u) = \begin{cases} (u+1)/2 & \text{for } u > 0 \\ (u-1)/2 & \text{for } u < 0 \end{cases}$$

and  $\underline{e}$  as in the attraction model above. The function  $G$  ensures that velocities of individuals equilibrate around either -1 or 1. Figure 5.4 gives examples of simulations of this model for different numbers of individuals. As density increases collective motion emerges in the form of a single large group of individuals all going in the same direction.

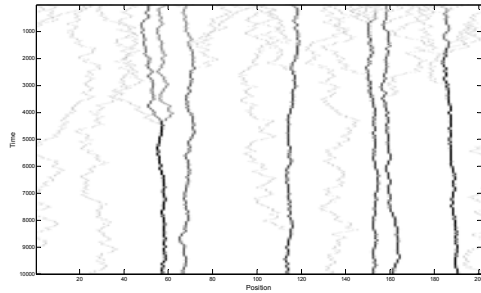
In two dimensions, Vicsek et al. (1995)  $\underline{s} + \underline{e}$  to be a unit vector with direction given by the average angle of the vectors plus some random term. Specifically,

$$\underline{s} + \underline{e} = \begin{pmatrix} \cos\left(\sum_{j \in R_i} \theta_j(t) + \varepsilon\right) \\ \sin\left(\sum_{j \in R_i} \theta_j(t) + \varepsilon\right) \end{pmatrix}$$

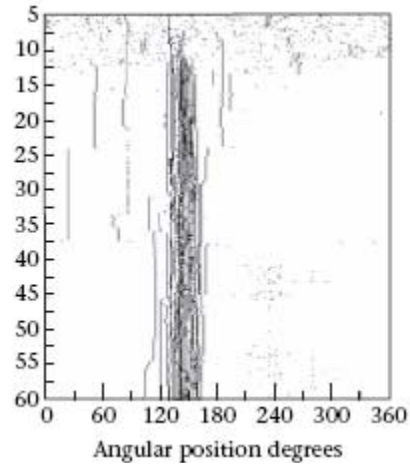
where the  $\theta_j$  are the directions of  $i$ 's neighbours and  $\varepsilon$  is chosen uniformly at random from a range  $[-\eta/2, \eta/2]$ . Unlike the two models above, in Vicsek's model  $\alpha=0$ , but the individual  $i$  is always included in the in the set  $R_i$  of neighbours. Thus each individual includes itself as a neighbour when averaging velocities. Figure 5.7 gives snapshots of simulations of this model for different magnitudes of noise. Noise plays the opposite role of density: for higher noise motion is less ordered.

**Repulsion, attraction, alignment and blind angles:** Couzin et al. (2002) model involves three zones of interaction: an inner zone of repulsion, an intermediate zone of orientation and an outer zone of attraction (Figure 5.8a). The individuals have a blind angle behind them within which they do not respond to individuals which would otherwise be in their orientation or attraction zone. The rule for repulsion is simply that individuals move directly away from nearby individuals. The rules for attraction and alignment are similar to those described for the two simple models. Figure 5.8 investigates a three dimensional version of this model for different sizes of orientation zones. Provided there is a sufficiently large blind angle, the group goes through a transition from swarm to milling torus to a highly aligned group.

(a)



(b)



(c)

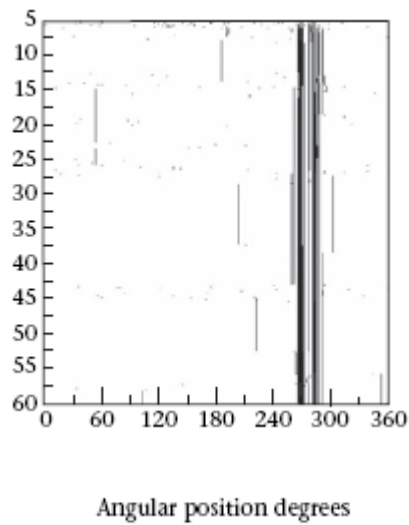


**Figure 5.2:** Outcome of (a) simple attraction model in Box 5.B compared to (b) experiments on cockroach aggregation and (c) Jeansson et al. (2005) detailed individual-based model.

Such aggregation dynamics are seen in cockroach groups (Jeanson et al. 2005). Cockroaches interact via antennal contact and are attracted to other cockroaches through physical contact. Thus, relative to the size of their environment, their zone of attraction is small. Jeanson et al. (2005) placed small

groups of cockroaches in a circular arena and watched their aggregation behaviour. Since cockroaches are strongly attracted to walls, most of their movement is constrained to the edge of this arena. In effect, the attraction to the arena edge means that movements of the cockroaches take place in one dimension and the aggregation process can be visualised by plotting the angular position of the cockroaches through time (figure 5.2b). In experiments where cockroaches were initially placed at random within the arena, a cluster quickly formed containing nearly all of the cockroaches. As in the SPP model, cockroaches within the cluster move much less than those outside of it.

Jeanson et al. (2005) developed a parameterised model based on experiments on groups of two to four cockroaches. The principle underlying this model was similar to the simple aggregation SPP model, but it included more detail of walking trajectories in different parts of the two-dimensional arena, probabilities of individuals starting and stopping walking, and the effect of collisions from different directions such as front and behind. The model showed that local contacts alone were sufficient for the rapid aggregation observed in experiments (figure 5.2c).

Whether animals aggregate depends on their environmental context (Krause 1994; Krause & Ruxton 2002). Larger groups provide dilution from predator attack and individuals in smaller groups get a larger share of food discoveries (chapter 2). Hoare et al. (2004) found killifish group sizes were significantly smaller in the presence of food odour and larger in the presence of an alarm odour. To explain the behavioural mechanisms that produced these observations they used an SPP model of fish interactions, with terms for repulsion, attraction and alignment. They showed that the observed change in group size distribution could be explained solely by a change in the size of the interaction zone. The distance at which a fish is attracted to another fish decreases in the presence of food and increases in the presence of a predator. This study provides a nice link between mechanism and function: the regulation of group sizes to perceived risk results directly from a change in interaction radius.

The mechanisms underlying spatial aggregation have been studied for a range of species: from midges (Okubo & Chiang 1974) and bark beetles (Deneubourg et al. 1990b) to primates (Hemelrijk 2000). More than twenty years since its publication, the review by Okubo (1986) still provides the best synthesis of mathematical and empirical aspects of aggregation.



## 5.2 Alignment

Attraction alone cannot explain the dynamics of most animal flocks. In particular, the aggregative clusters formed by between-individual attraction move slower as cluster size increases (figures 5.1a and 5.2a,c). These observations are in direct contrast to those of fish schools, locust swarms and migratory birds that, while remaining a cohesive group, move rapidly in the same direction. Indeed, it is the rapid propagation of directional information that characterises these groups, and

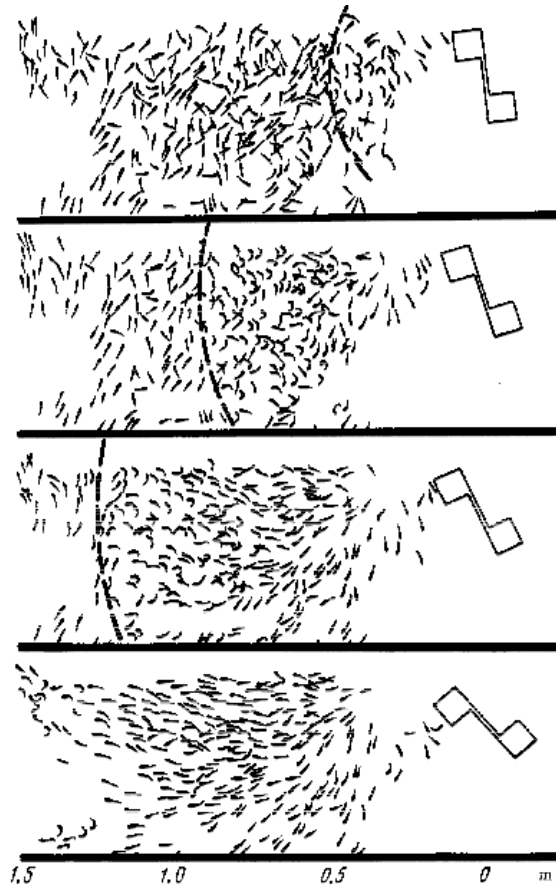


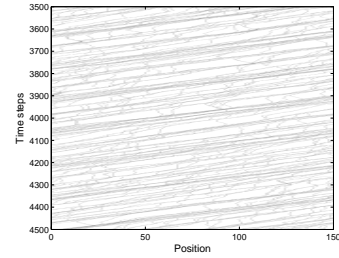
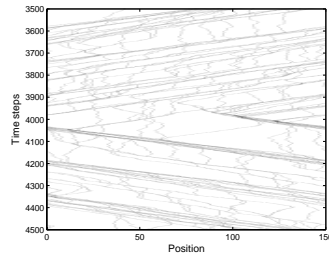
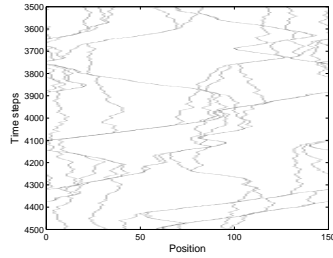
**Figure 5.3:** Example of Radakov's experiment where fish schools are presented with a **fright stimulus**. The position of fish was filmed and projected on a wall so that a picture could be made of the position and orientation of the fish. Reproduced from Radakov 1973.

poses the greatest challenge to our understanding of them (Couzin & Krause 2003). How is it that a bird flock or a fish school can apparently turn in unison such that all members almost simultaneously change direction?

It was the pioneering experimental work by Radakov (1973) that first showed how changes in direction can be rapidly propagated by local interactions alone. He used an artificial stimulus to frighten only a small part of a school of silverside fish. The fish nearest to the stimulus changed direction to face directly away from it. As these fish changed direction they stimulated others nearby, but further away from the artificial stimulus, to also change direction. A “wave of agitation” spread away from the artificial stimulus (figure 5.3). This propagation of directional information was much more rapid than the displacement of the fish. The fish nearest to the stimulus moved less than 5cm in the same time it took every fish within 150cm of the stimulus to change direction to face away from the stimulus. Changes in direction (a)

(c)

(b)



(d)

(e)

(f)

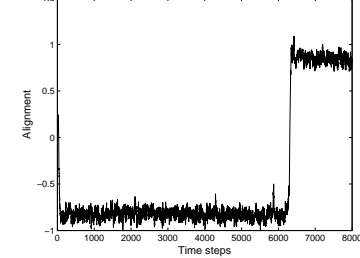
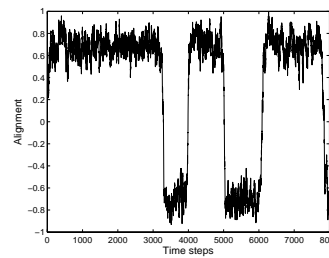
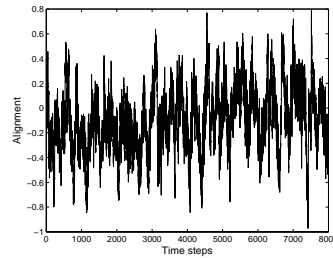


**Figure 5.4: Example simulations from one dimensional SPP models.** Simulation of the SPP model of alignment in one dimension. The change in particle density through time for (a)  $N=10$  (b)  $N=50$  and (c)  $N=100$  particles. The alignment at time  $t$  is defined as

$$\frac{1}{n} \sum_{i=1}^n u_i(t)$$

The average direction. The alignment is given for (d)  $N=10$  (e)  $N=50$  and (f)  $N=100$  particles. Other parameters are  $L=150$ ,  $r=1$ ,  $v=1$ ,  $\alpha=0.66$  and  $\eta=0.8$ .

propagated at speeds of up to 11.8 – 15.1 metres per second over distances of between 30 and 300cm.

While not directly inspired by Radakov's work, the transfer of directional information was the key ingredient in the self-propelled particle models of Vicsek et al. (1995). In fact, Vicsek's model has only two ingredients determining the direction particles move in: alignment to nearby particles and noise (Box 5.B). Figure 5.4a-c shows examples of these simulations in one dimension for different particle densities. A central prediction of Vicsek's model is that as the density of particles increases, a transition occurs from disordered movement to highly aligned collective motion (Czirok et al. 1999; Czirok et al. 1997; Vicsek et al. 1995). Figure 5.4d-f show how the mean direction, or the degree of alignment, of particles changes through time in a one dimensional version of the model from Box 5.B for three different particle densities. At low densities, the alignment remains close to zero (figure 5.4a,d). At intermediate densities, all particles adopt a common direction for a period of time but this direction switches at random intervals (figure 5.4b,e). At high densities, particles adopt a common direction which persists for a long period of time (figure 5.4c,f). The transition from disorder (random motion) to order (aligned motion) occurs at a critical density, below which alignment is zero and above which absolute alignment increases with group size (Czirok et al. 1999).

Such a transition from disordered to ordered motion is seen in the collective motion of locusts. Buhl et al. (2006) looked at the alignment of various densities of locusts in an experimental ring-shaped arena. This setup effectively confined the locusts to one dimension and the degree of alignment could be measured as the average direction of movement relative to the centre of the arena. For small populations of locusts in the arena there was a low incidence of alignment among individuals. Where alignment did occur, it did so only after long initial periods of disordered motion (figure 5.5a). Intermediate-sized populations were characterized by long periods of collective rotational motion with rapid spontaneous changes in direction (figure 5.5b). At large arena populations, spontaneous changes in direction did not occur within the time scale of the observations, and the locusts quickly adopted a common and persistent direction (figure 5.5). As predicted by Vicsek's model, alignment of locusts

becomes non-zero above a critical density (figure 5.6). The simplicity of Vicsek's SPP model suggests that phase transitions should be a universal feature of moving groups (Buhl et al. 2006). Similar transitions are observed in fish (Becco et al. 2006) and in tissue cells (Szabo et al. 2006).

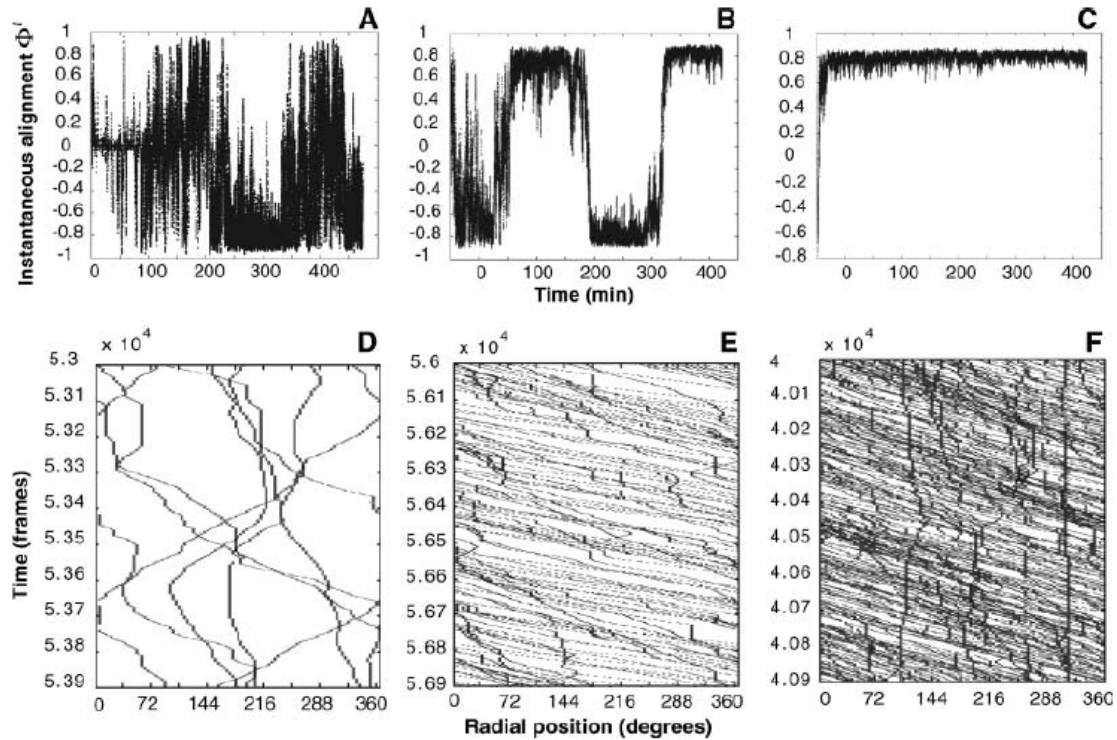


**Figure 5.5: Experiments on locusts in a ring.** The alignment over the experiment of (a) 7 locusts, (b) 20 locusts and (c) 60 locusts. (d to f) Corresponding samples of time-space plots (3 min), where the x axis represents the individuals' angular coordinates relative to the center of the arena, and the y axis represents time. Reproduced from Buhl et al (2006).

When extended to two or three dimensions, Vicsek's model generates spectacular dynamical patterns that are highly reminiscent of the movement of flocks (figure 5.7). Again the two dimensional model undergoes a phase transition where alignment becomes non zero above a critical particle density or below a critical noise level (Vicsek et al. 1995).

While reproducing many of the characteristics of animal flocks, Vicsek's model is by no means sufficient to explain all aspects of flocking. To start with, it does not contain an attraction term of the type discussed in the previous section. In fish, attraction between individuals has long been viewed as having equal importance to alignment in determining group dynamics (Partridge 1982). The omission of attraction from Vicsek's model means that a bounded group cannot form. In an SPP model without an attraction term, a large group of particles moving in the same direction spreads out and particles will 'escape' from the back of the group (Gregoire et al. 2003). When confined to a small space this

diffusion will not lead to a significant breakup of the group because stragglers are picked up when they meet the large group again, but in an infinite (or large) space the group will eventually break apart.

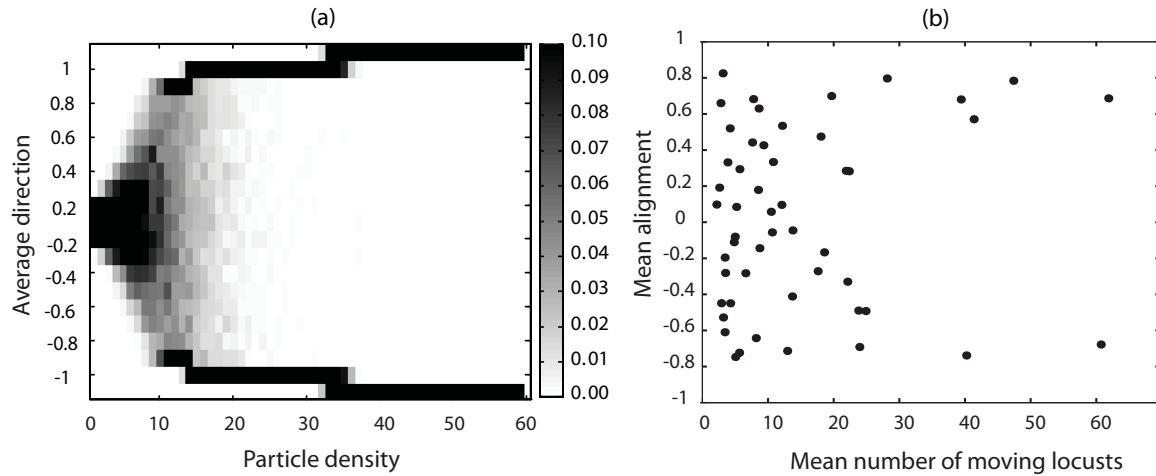


**Figure 5.6:** Comparison of the mean alignment in the (a) SPP model and (b) the locust data as a function of the number of particles (or locusts). Reproduced from Buhl et al (2006).

A cohesive moving group can form if both attraction and alignment terms are included in an SPP model. Gregoire et al. (2003) drew a phase diagram for a two-dimensional SPP model which included terms for attraction, alignment and noise. They found that when attraction was weak relative to alignment, particles behaved as either a disordered or moving 'gas', similar to those seen in the two-dimensional Vicsek model (figure 5.7). This gas was characterised by the proportion of particles that were members of the largest group being less than one. When attraction was increased the proportion of particles within the largest group tended to one, and Gregoire et al. classified this state as a liquid 'droplet'. Within this droplet two close together particles diffused away from each other through time while remaining within this large group. Compared to the gas in figure 5.7, in which groups split apart and reform, individuals moved around within the single droplet but did not leave it. As the attraction term was further increased, the liquid turned into a solid 'crystal' and the particles remain at a fixed position within the crystal through time. Provided alignment was sufficiently large relative to noise, both liquids and solid exhibited cohesive collective motion where all particles moved as a group in the same direction.

A number of aspects of Gregoire et al.'s model resemble the motion of animal flocks. Moving crystals and droplets both exhibit periods of ballistic flight, where the mean square displacement of the group was proportional to  $(\text{time})^2$ , i.e. groups fly in a straight line. Furthermore, the lengths of these ballistic flights increased with the size of the group. This is in contrast to the non-moving phases where attraction is dominant, e.g. as in figure 5.2a. In this case, the mean square displacement of the group was proportional to time and the lengths of ballistic flights decreased inversely (a) (b)

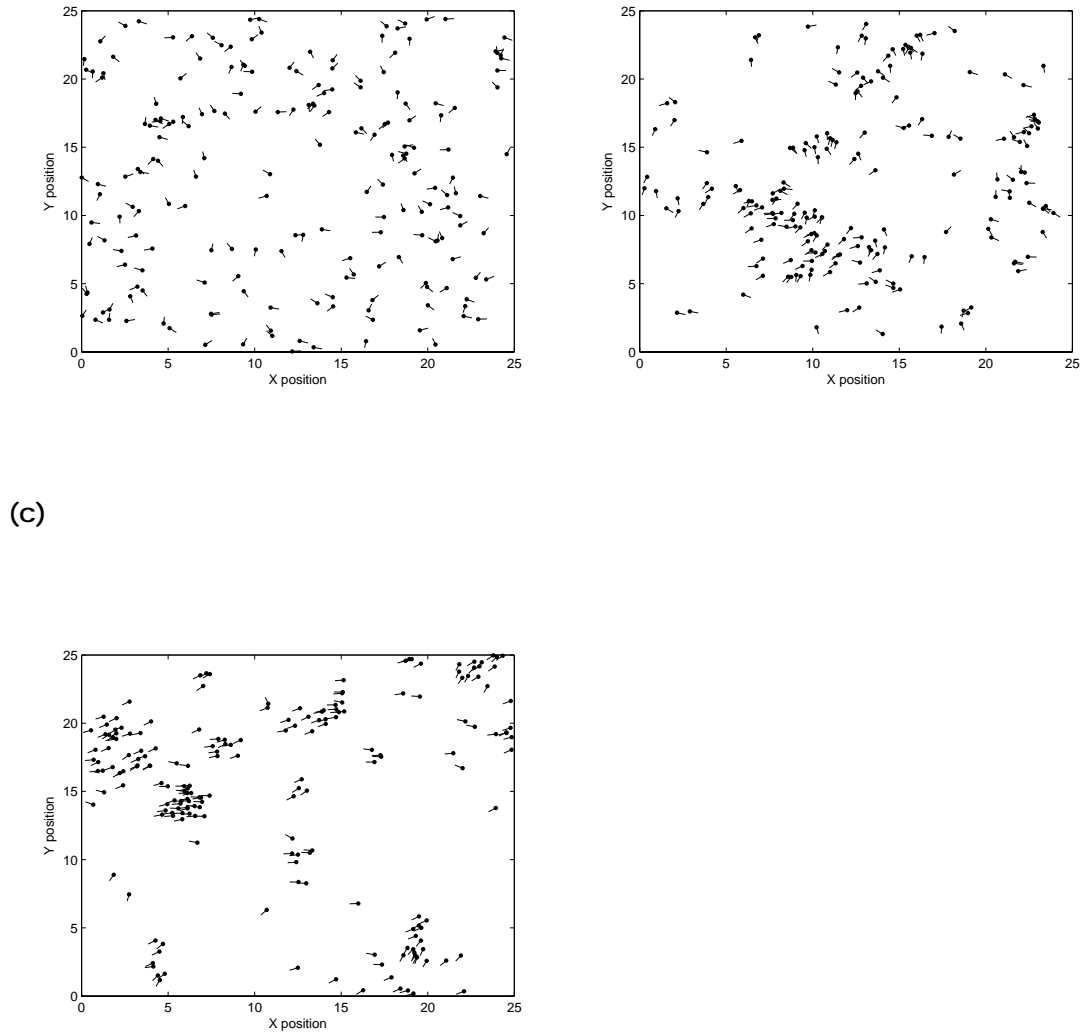


**Figure 5.7: Example of patterns from two dimensional SPP model with alignment.** Model is as described in box 5.B. Parameters are  $n=200$ ,  $v_0=0.5$ ,  $L=25$ , and  $r=1$ . The noise is varied between simulations (a)  $\eta=3$ , (b)  $\eta=1.5$  and (c)  $\eta=0.5$ .

proportionally to group size. Crystals and droplets both resemble various forms of moving animal groups: crystals look roughly like highly parallel groups of fish or birds, while the droplets possibly resemble flying locust swarms. Particularly interesting is the existence of mesoscopic “hydrodynamical” structures, such as jets, vortices, etc., within droplets (Gregoire et al. 2003). It is this dynamical patterning on a meso-scale within a generally coherent motion on the scale of the entire group that might be said to best characterise the collective motion of many flocking animals. However,

the ‘zoology’ of these meso-scale shapes has not been fully investigated and compared to empirical observations.

### **5.3 Rules of motion**

The attraction and alignment models discussed in the previous sections have not been calibrated against real data of how fish, birds or locusts interact with one another. Instead, the philosophy of these models is to provide as simple as possible model for the interaction of animals that reproduces the key features of flocks. This philosophy is aimed at ensuring that model outcomes are not dependent on some particular biological feature, but reveal universal properties of all flocks. The approach is also to some degree unavoidable. Empirical determination of the detailed interactions of fish or birds is technically difficult. These groups move in two or three dimensions and often come in close contact with each other, making automated or even manual tracking difficult (Hale 2008).

There are, however, a number of high quality studies of fish interactions, most notable those of Partridge in the early 1980s. Studies of the structure of schools of saithe, cod and herring show that fish maintain a minimum distance between each other, supporting evidence for local repulsion (Partridge et al. 1980). By tracking individual fish, Partridge (1981) established that saithe match their swimming direction and speed to their two nearest neighbours, but probably not to more distant neighbours. Partridge & Pitcher (1980) found that ‘blindfolded’ saithe continued to match short term changes in velocity of their neighbours using their lateral line (the motion detecting sense organ which runs down fish bodies). Vision was however important in maintaining between neighbour distance, with blind fish having increased nearest neighbour distances. Fish which had their lateral line disabled compensated by changing position so they could see direction changes by neighbours. In general, the lateral line appears to determine alignment, while vision determines attraction and repulsion.



An impressive step forward in the understanding of both the global structure of groups moving in three dimensions and the behaviour of individuals within these groups is the Starflag project (Ballerini et al. 2008a; Cavagna et al. 2008a; Cavagna et al. 2008b). Using multiple cameras these researchers were able to determine the position of most of the starlings in flocks consisting of thousands of birds. Like fish, the starlings maintain a minimum distance from each other, i.e. have a zone of repulsion (Ballerini et al. 2008a). Starlings are also less likely to have neighbours behind or in front of them than to have neighbours on either side. As distance from a focal bird increases this spatial organisation disappears, so that birds further away from a focal bird are equally likely to be at any angle.

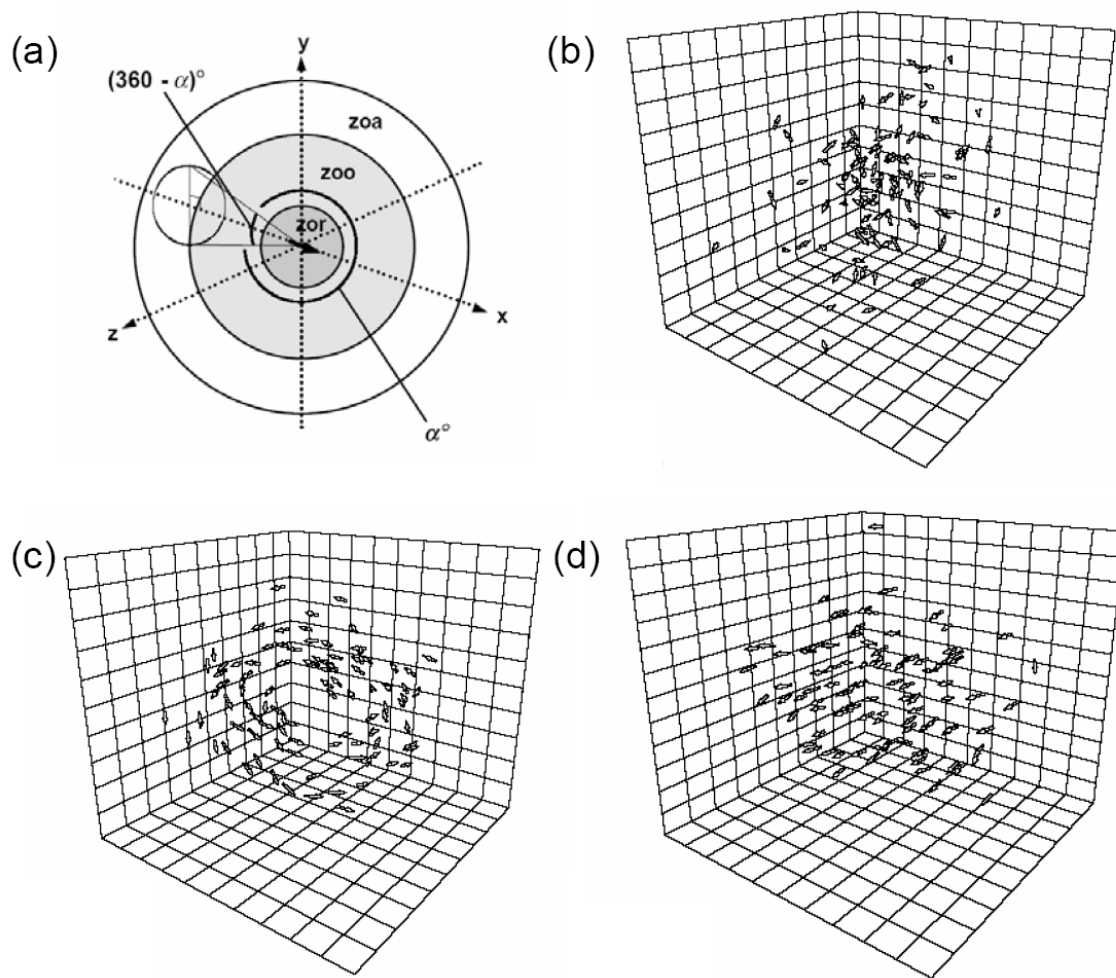


**Figure 5.8: Transition from swarm to torus to alignment.** (a) Illustration of the rules governing an individual in the fish model. The individual is centred at the origin: zor, zone of repulsion; zoo, zone of orientation; zoa, zone of attraction. The possible 'blind volume' behind an individual is also shown, a, field of perception. Collective behaviours exhibited by the model: (b) swarm, (c) torus and (d) dynamic parallel group.

Local spatial structure is not simply a function of distance but rather a function of neighbour number. The nearest neighbour is much more likely to be to the side of than directly in front of or behind a focal bird. This tendency then decreases for the second neighbour then the third neighbour and so on. After the sixth or seventh neighbour the spatial structure vanishes and these neighbours are equally likely to be at any angle relative to the focal bird (Ballerini et al. 2008b). This relationship is less robust when considering only the distance between neighbours. Even when the flock is more tightly packed spatial correlations are seen only between a fixed number of neighbours. The relationship would suggest that instead of interacting with all or some birds within a certain fixed radius, as is assumed in most models, starlings interact with their 6 or 7 nearest neighbours.

## **5.4 Complex moving patterns**

The shapes of bird flocks, fish schools and locust swarms are not limited to groups of aggregated or aligned individuals. Some of these shapes can emerge from simple interactions of repulsion, attraction and alignment alone. For example, Couzin et al. (2002) proposed a model in which individual animals have three zones—repulsion, alignment and attraction—of increasing size, so that individuals are attracted to neighbours over a larger range than they align, but decrease in priority, so that an individual always moves away from neighbours in the repulsion zone (figure 5.8a). These individuals also have a rear blind zone within which they cannot sense others.

Keeping the repulsion and attraction radii constant, Couzin found that as the alignment radius increased, individuals would go from a loosely packed stationary swarm (figure 5.8b), to a torus where individuals circle round their centre of mass (figure 5.8c) and, finally, to a parallel group moving in a common direction (figure 5.8d). This transition from milling to torus to departure is typical of the motion of real fish schools. The model shows that these three very different collective patterns self-organise in response to small adjustments to one factor: the radius over which individuals align with each other.

Other patterns seen in animal flocks may be more difficult to produce from models of identical 'memoryless' self-propelled particles interacting in a homogeneous environment. For example, Radakov (1973) reports "feeler" structures in silverside fish during their evening migration away from the shore. A

few fish swim away from the group forming a ribbon-like structure as others follow. The leading group then reduces speed and starts feeding, at which point a "neck" builds up as more and more fish are drawn from the main group. In some cases this neck leads the whole group to the new feeding ground, while in others the neck breaks off and a sub-group separates from the main group. Overall, the process gives the impression of the school making a tentative investigation of whether it is worth moving feeding grounds.

Another common pattern in fish schools is the fountain response to the approach of a predator towards a group of prey (Pitcher, 1985). In this response the fish fan out in front of a predator and circle round behind it. Self-propelled particle models can reproduce this type of group response to predators (Iwamoto, 2001 and see section 5.6). However, Hall et al. (1986) argue that a fountain response can occur simply by each individual prey moving away from the predator while keeping it at the edge of its field of view. Fish have a blind angle of roughly  $60^\circ$ , so by keeping the predator behind them at an angle of  $150^\circ$  the fish are moving away from the predator as rapidly as possible without losing sight of it. This argument appears consistent with experimental data on the response of shoals of juvenile whiting (Hall et al. 1986), but it is not entirely clear whether social interactions may also play a role in creating the fountain effect.

Determining the degree to which simple rules for attraction and alignment capture the shapes produced by real animal groups remains a key problem (Parrish et al. 2002).

No detailed statistical comparison has been made between the motion of and within real flocks and those predicted by SPP models. For example, Uvarov (1977), describes the marching bands of locusts as having a dense front and columns that go through an otherwise diffuse cloud of individuals. These observations have little in common with the shapes arising from, for example, Gregoire et al.'s (2003) model. Similarly, Ballerini et al.'s (2008) observation that starling flocks have a dense boundary and a sparser interior directly contradicts most SPP models, which predict either homogeneous density within a group or a density which decreases with distance from the group's centre. Explaining the emergence of complex moving structures will require greater consideration of the rules adopted by individuals, of how individuals interact with the environment and of between-individual differences.

## **5.5 Decisions on the move**

When navigating, animals in moving groups usually have access to two types of information, their own experience or internal compass information and the direction taken by other group members. A central problem faced by animals travelling in these groups is how to integrate this information, especially when members cannot assess which individuals are best informed. In the context of avian navigation, two alternative schemes have been proposed (Wallraff 1978). The “many wrongs” hypothesis, which is described in more detail in section 4.3, is that individuals average their preferred direction, leading to a compromise in route choice. The average of these many wrongs should lead to an improvement in navigational performance. Wallraff's alternative to the many wrongs hypothesis is the 'leadership' hypothesis. Under this hypothesis, one or a small number of the animals takes a leading role and the others follow.

Neither the many wrongs nor the leadership hypothesis accounts for how information is transferred between group members through local interactions. Indeed, the many wrongs hypothesis leads to the paradox, discussed in section 4.4, that for information to be transferred some individuals must follow others but at the same time too much following will reduce the success of the averaging. To bypass this limitation, Biro et al. (2006) developed a mechanistic model of navigational conflict between pairs of individuals. In the model (described in Box

5.C), individuals

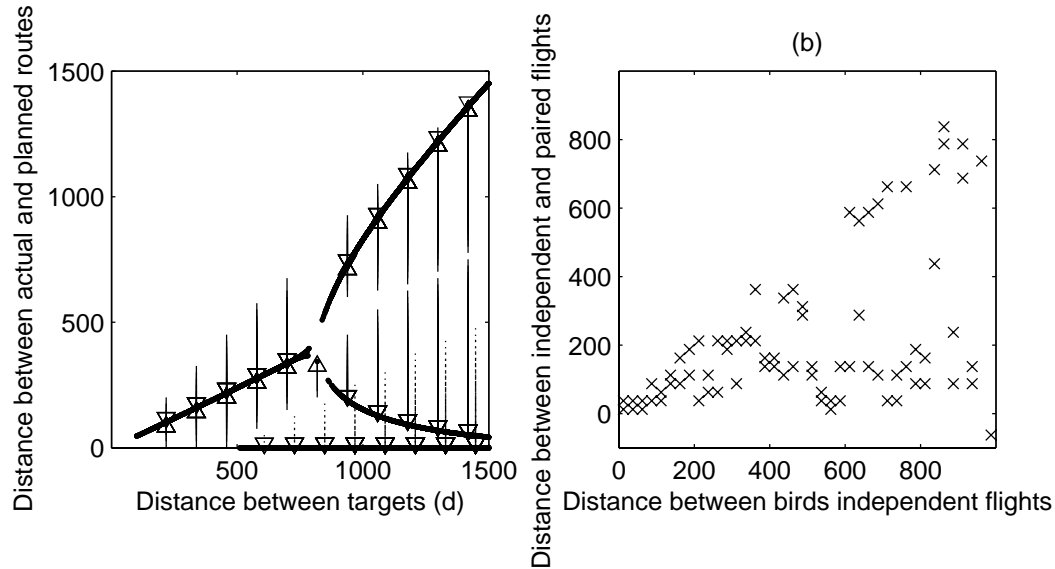


**Figure 5.9: Outcome of decision-making in pairs.** (a) Predictions model in box 5C. Equilibrium solutions of equations 5.C.3 and 5.C.4 as a function of the distance between the individuals' targets,  $d$ . The arrows show how different initial positions of bird X lead to different equilibria. The initial position of bird Y is always  $d/2$ . The parameter values are  $r_a = 400$ ,  $r_b = 80$  were chosen to reflect the perception ranges of real pigeons. The other parameters  $\alpha=1$  and  $\beta=1$  assume no intrinsic difference between the birds (b) Outcome of pigeon experiments. Point by point distances between each birds established route and its route taken when in a pair are made in to a histogram and then the largest and the second largest modes of the data are plotted.

interact according to two hypothesized forces: attraction to its own target position (own information) and attraction to the partner's current position (social information).

Figure 5.9a shows, for the model in Box 5.C, the effect of varying the distance between the individuals' targets,  $d$ , on the final decision reached. The model predicts that at small distances between established routes, individuals average,

with their position equilibrating at  $d/2$ . At a critical between-route distance, of approximately twice the range at which individuals are maximally attracted to their

### Box 5.C Model of paired navigational decision-making

We consider a dynamic model for decision-making, where two individuals, X and Y each decide on a real-valued 'position', starting from initial positions  $x(0)$  and  $y(0)$ . These individuals come to a final position as a result of a combination of two forces: predisposition to move toward a target position and local attraction towards the other individual's current position.

**Predisposition to target:** X, respectively Y, are attracted to a target position with value 0, respectively  $d$ . The rate at which an individual moves toward its predisposed choice initially increases with distance from the target, but above a point of maximum attraction the rate decreases. For individual X, we model this rate with the function

$$-x \exp(-x/r_a) \quad (\text{equation 5.C.1})$$

where  $x$  is the current position and  $r_a$  is the point at which the attractive force towards the target reaches a maximum. Individuals further from the target than  $r_a$  have a weaker attraction towards it due to difficulties in perceiving the target, while individuals nearer than  $r_a$  have a decreasing but positive attractive force, modelling an increasing degree of 'comfort' with decreasing distance to the target.

**Between-individual attraction:** We model this with the function

$$(x-y) \exp\left(-\left(\frac{(x-y)}{\sqrt{2}r_b}\right)^2\right) \quad (\text{equation 5.C.2})$$

where  $x$  and  $y$  are the current positions of the two individuals and  $r_b$  is the point of maximum attraction to other individuals. Attraction only occurs locally, so that once individuals move out of the range of perception, the rate of attraction quickly decreases.

We combine the two forces acting on the individuals to give a differential equation model of how the individuals change position:

$$\begin{aligned} \frac{dx}{dt} &= -x \exp(-x/r_a) - \alpha (x-y) \exp\left(-\left(\frac{(x-y)}{\sqrt{2}r_b}\right)^2\right) \\ \frac{dy}{dt} &= \beta (d-y) \exp(-(d-y)/r_a) + \alpha (x-y) \exp\left(-\left(\frac{(x-y)}{\sqrt{2}r_b}\right)^2\right) \end{aligned}$$

(equations 5.C.3 and 5.C.4)

The parameter  $\alpha$  determines the ratio of the maximum between-individual attraction over the maximum attraction to the target.  $\beta$  determines the ratio (Y:X) of the strength of the individuals' attraction to their targets. Figure 5.9a shows the equilibrium solutions to the model equations as a function of the distance  $d$  between the individuals' targets.



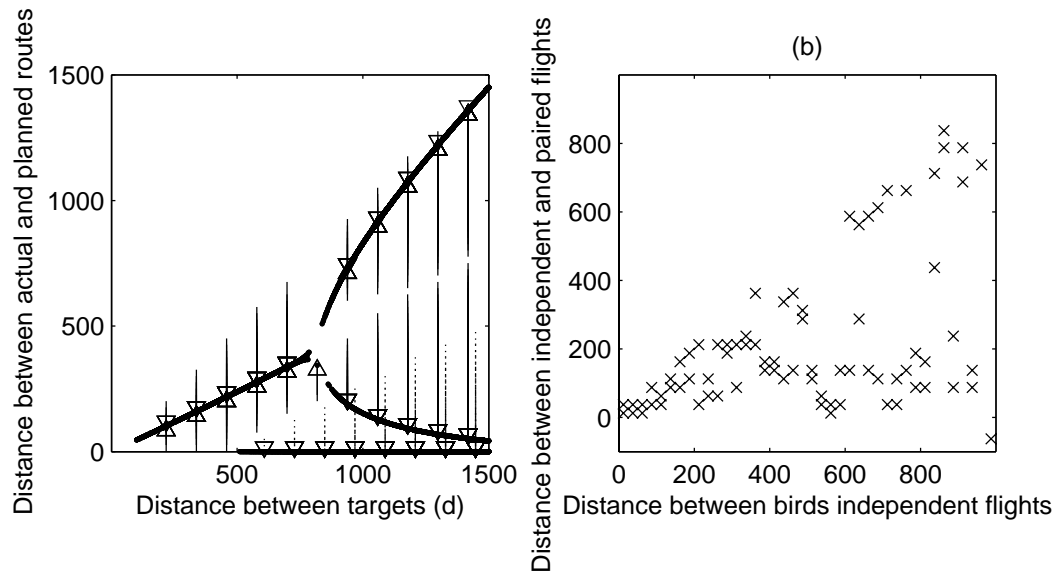


**Figure 5.9: Outcome of decision-making in pairs.** (a) Predictions model in box 5C. Equilibrium solutions of equations 5.C.3 and 5.C.4 as a function of the distance between the individuals' targets,  $d$ . The arrows show how different initial positions of bird X lead to different equilibria. The initial position of bird Y is always  $d/2$ . The parameter values are  $r_a = 400$ ,  $r_b = 80$  were chosen to reflect the perception ranges of real pigeons. The other parameters  $\alpha=1$  and  $\beta=1$  assume no intrinsic difference between the birds (b) Outcome of pigeon experiments. Point by point distances between each birds established route and its route taken when in a pair are made in to a histogram and then the largest and the second largest modes of the data are plotted.

established routes, a bifurcation occurs. For  $d$  larger than this critical value, both individuals move closer to that of one of the individuals. A third possible outcome is splitting, where each individual moves exclusively towards its own target. Such outcomes occur over a wide range of  $d$  but always result from initial differences in the individuals' positions.

While the model in Box 5.C provides an abstract representation of navigational decision-making, it was designed specifically with the behaviour of homing pigeons in mind. Predisposition to a target models the phenomenon of route

recapitulation and route loyalty by homing pigeons and between-individual attraction models social cohesion between birds. We tested the model's predictions against data we collected on homing pigeons (Biro et al. 2006). We first allowed homing pigeons to each establish their own route home from a release site. Once individuals had learnt their own routes they were released in pairs. In these paired releases instances of many wrongs compromise and of leadership were observed, even within a single journey of a single pair of birds.

In order to test how the distance between the birds' 'target' routes affected the outcome of their paired flight, we looked point-by-point through the whole flight at how the distance between the birds' independent flights affected the distance between their routes. Figure 5.9b shows the largest and second largest modes of distances between routes taken by individuals during their paired flight and the immediately preceding single (established) route as a function of distance between the birds' established routes at the corresponding point of the journey. We see a similar bifurcation in this data as we see in the model prediction (figure 5.9a). As the distance between the birds' targets increases a bifurcation occurs from compromise to leadership.

Our model is limited because it deals with only two individuals and abstracts away possibly important aspects of spatial interactions. Couzin et al. (2005) proposed an SPP model where individual particles move in a two dimensional space according to rules of attraction, alignment and repulsion. In this model a large group of 'uninformed' individuals interacts with two small groups of informed individuals which each move toward different targets. As the angle between the targets increases there is a bifurcation where the group goes from taking a direction intermediate to the two small leading groups to taking the direction preferred by one of the two groups.

## **5.6 Leading the swarm**

An interesting prediction of the Couzin et al. (2005) model is that a small number of informed individuals can lead a large group. In these simulations groups of 200 uninformed individuals were almost always successfully led to a target by groups of less than 10 leaders. Thus observations of large numbers of birds, fish or insects moving in the same direction do not imply that even a majority of individuals know where they are going or even know which individuals know where they are going. The Couzin et al. (2005) model thus suggests a 'subtle guide' mechanism:

a largely uninformed group can be led by a small group of informed 'leaders' even when the identity of the leaders is unknown.

One of the most impressive examples of a large group of uninformed individuals being led by a small group is the flight of honey bee swarms from their temporary bivouac on a tree branch to a new nest site (see section 9.3). Up to around 10,000 bees of which only 2 or 3% are informed of the location of the nest site fly as a single swarm to the site. How does such a small group lead such a large group to a small nest site? Lindauer (1955) hypothesised that the informed individuals repeatedly 'streak' through the swarm in order to inform the other bees of the direction of the nest. Janson et al. (2005) formalised this hypothesis in an SPP model and showed that 150 'streaker bees' could lead a swarm of 3,000 uninformed bees, and these swarms could avoid obstacles in their path without splitting. While streaking might help guide a swarm, the 'subtle guide' hypothesis presented above suggests that streaking is not a requirement for a small number of individuals to lead a large swarm. A further alternative to the 'subtle guide' or 'streaker bee' hypotheses is a 'vapour trail', where the informed bees move to the front of the swarm and release a chemical pheromone creating a gradient which the other bees follow (Avitabile et al. 1975).

Beekman et al. (2006) tested the 'vapour trail' hypothesis by sealing, in the bees, the glands which release pheromone and comparing the flight of sealed gland colonies with control colonies. Gland sealing had no significant effect on the flight speed of the swarm nor on the time it took the swarm to reach a nest box, contradicting hypotheses based on pheromones. Beekman et al. (2006) noted that some bees in the swarm were moving at maximum speed (9-10m/s) while the swarm as a whole moved at only 2-3 m/s, providing evidence for the 'streaker bee' hypothesis. Schultz et al. (2008) provided stronger evidence of streaking by filming a swarm from below. They found that bees in a top portion of the swarm flew quickly in the direction of the nest site and these fast moving bees were observed at the front, middle and back of the swarm. However, while it appears clear that some bees streak along the top of the swarm and then return through it at slower speeds, there is still no direct link between these fast flying bees and the scouts.

## 5.7 Evolution of flocking

Hamilton (1971) and Vine (1971) were the first researchers to look at how the geometry of an animal group might be shaped by natural selection. They both proposed 'selfish herd' models in which individuals in the group are motivated to move into the centre of the group by the risk of predation. In Hamilton's model, individuals live on a one-dimensional lattice and follow the rule: if the site an individual occupies has a larger population than those to the left and right then it stays there, otherwise it moves to the neighbouring site that is occupied by the largest number of other individuals. In contrast to the mechanistic model of aggregation described in Box 5.A, Hamilton's model is motivated by functional considerations. However, the outcome of both models is similar: tightly packed clumps of individuals emerge (as they do in figure 5.2a). Vine and Hamilton both expand on this initial model and find similar results: tight aggregations are a consequence of selfish individuals' attempt to use other individuals as cover.

The geometrical predictions of selfish herd models hold for a wide range of species that form stationary groups (Krause 1994; Krause & Ruxton 2002; Quinn & Cresswell 2006; Rayor & Uetz 1990). Individuals near the centre of these groups are less likely to be attacked than those on the edge. Several studies have revealed that when there is a predation risk, fish move closer together (Krause 1993; Tien et al. 2004). On the other hand, Focardi & Pecchioli (2005) found that the foraging success of deer increased with distance from the centre of the group. There is thus a trade-off between increased food intake on the outside of the group and increased safety in the centre. We might then expect position in a group to be determined by nutritional state, with well fed individuals near the centre and hungry individuals on the outside.

In moving groups it is less clear how the position in a group relates to safety from predation. Parrish (1989) showed in laboratory experiments that while grouping silverside fish are attacked less often by sea bass than stragglers which have recently departed from the group, if the group is attacked it is the fish in the centre that are the subject of these attacks. Parrish suggested that this is because the predators attack the centre of the group, which then splits in two leaving central individuals exposed. This interpretation is supported by simulations of SPP models (Inada & Kawachi 2002). Parrish's study is limited however by the fact that very few attacks by the predators were successful: only five group members were killed throughout all experiments, three of which were in the centre and two on the periphery.

The complex dynamic patterns generated by flocking animals should convince us that a selfish desire to be shielded by others is not the only evolutionary force that has shaped them. Group membership may also allow individuals to gain information about the location of food (Pitcher et al. 1982) and of predators (Treherne & Foster 1981), to benefit in terms of energetic efficiency (Weimerskirch et al. 2001) and even to hunt co-operatively (Partridge et al. 1983). A problem however is disentangling functional and mechanistic explanations for dynamic patterns. Many patterns may be a consequence of the interactions between individuals and have little or no adaptive significance (Parrish et al. 2002). For example, the transition from disorder to order in locust marching appears to be a fundamental property of SPP models, suggesting that rather than resulting from the fine tuning of natural selection it is simply a necessary aspect of all grouping animals (Grunbaum, 2006). Similarly, it would be wrong to conclude that a moving fish torus has evolved to signal between group members that departure is imminent, but rather it could be an unavoidable consequence of all members increasing their tendency to align with each other (Couzin & Krause 2003).

Behaviours which produce flocking patterns are in some cases themselves subject to natural selection. For example, one intrinsic property of SPP models is dynamic instability. Such instability was seen at intermediate densities in experiments on locusts, with changes in direction rapidly spreading through the entire group (figure 5.5e). If a small number of locusts spontaneously change direction, the others rapidly change their direction in response. This spread of directional information is reminiscent of Radakov's (1973) experiments on fish. Information about the presence of a stimulus is rapidly transmitted through the entire group.

Several modelling studies have investigated how the rules governing the alignment, repulsion and attraction of self-propelled particles might be optimised so as to allow the particles to avoid predation (Inada & Kawachi 2002; Lee 2006; Lee et al. 2006; Zheng et al. 2005). In these studies a predator particle that is introduced into the simulation attempts to attack the group of prey particles. Inada & Kawachi (2002) varied the maximum number of neighbouring individuals with which each prey aligned. They showed that if prey aligned with only one nearest neighbour then group movements were uncoordinated in response to a predator, but if they interacted with two or three the group was able to effectively align away from the predator. However, if prey individuals

align with larger numbers of neighbours then the group would change direction slowly in response to a predator, because the minority of individuals that had sensed the predator and begun to move away from it would be 'outvoted' by the uninformed majority that continue in their previous direction. Zheng et al. (2005) obtained similar results to Iwada by changing a different model parameter. They showed that there is an optimal weighting that individuals should put on aligning with other prey relative to orienting away from the predator. By aligning with each other rather than purely away from a predator, the prey avoid costly collisions. The collective outcome is a confusion effect, where the predator repeatedly changes target.

Most modelling studies of predator avoidance have looked at group success, measured in terms of number of group members captured by a predator, as a function of model parameters. From a functional viewpoint, however, the question is how individuals regulate their propensity to align, or their interaction range, or other aspects of their behaviour so as to minimise their own probability of being caught by the predator. While aligning with others may increase the confusion effect for the predator, the best strategy for a focal individual may be to move directly away from the predator. As a result a social parasitism dilemma arises: while co-operating individuals can generate a pattern which optimises group success, a defecting individual surrounded by co-operators can benefit to the greatest degree by not participating in the pattern. The pattern is then not evolutionarily stable (see chapter 10).

Wood et al. (2007) investigated the evolutionary stability of self-propelled particles to predation. They used the same model for particle movements as Couzin et al. (2002) but allowed the particles to evolve their interaction zones in response to predation. The main parameters governing the interaction zones are the relative size of the attraction,  $R_a$  and orientation zones,  $R_o$ , as well as the angle  $\theta$  over which the particles can 'see' their neighbours. The total area over which a particle could monitor its neighbours, i.e.  $\theta\pi R_a^2$  was fixed to a constant for all particles. This constraint means that their viewing area is restricted to a local neighbourhood of constant area. On the first generation a population of 80 individuals each with its own values of  $R_a$ ,  $R_o$ , and  $\theta$  was simulated for a sufficient number of time steps so as to allow a dynamic pattern to form. A predator, which attempted to capture the prey individuals, was then introduced into the simulation. After a fixed number of time steps those surviving individuals, i.e. those which had not been caught by the predator, went on to the next generation and those individuals that were caught were replaced by 'offspring' of the

surviving individuals. These offspring were subject to small mutations in the parameter values so that individuals with new values for  $R_a$ ,  $R_o$ , and  $\theta$  entered into the population.

There was a clear pattern in the evolution of the parameters. Firstly, the angle over which the particles could see evolved to be large,  $\theta \approx 280^\circ$  leaving a blind angle of  $80^\circ$ . This is reasonably close to the blind angle of  $60^\circ$  of many species of fish (Hall et al. 1986). The evolution of the small blind angle constrained the attraction radius  $R_a$  within which the orientation radius  $R_o$  was then free to evolve. Two evolutionary outcomes were possible for  $R_o$ , evolving either to be close to, but slightly larger than, 0 or to be close to, but slightly smaller than,  $R_a$ . In the first case the particles formed a slow moving milling group (figure 5.10a) while in the second they formed a fast moving dynamic group (figure 5.10b). Which of these outcomes evolves depends on the initial values of  $R_o$  within the population and the rate of mutation during selection. If  $R_o$  was initially large a dynamic group would evolve and if it was initially small a slow moving mill would evolve.

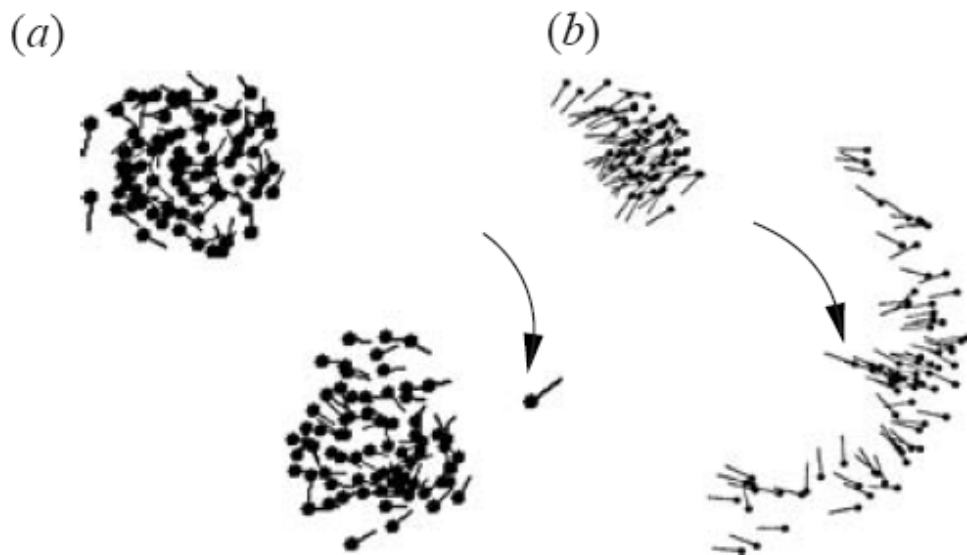


**Figure 5.10:** Typical example of the two types of evolutionarily stable flock types in the Wood et al. model. Each flock is shown before and during the attack of a predator. (a) is a compact milling torus that responds relatively slowly to the predator while (b) is a dynamic parallel group with a high degree of alignment but only loose between individual attraction. When a predator attacks the group fans out to avoid it. Prey heads are marked with a circle and the line indicates their current velocity. Predators are larger and marked with an arrow.

While both evolving through 'natural selection', the dynamic group was more efficient than the slow moving mill at avoiding predation. The dynamic group had similar responses to predators as the optimised groups of Inada & Kawachi (2002) and of Zheng et al. (2005). It produced a confusion effect and split to avoid predation in 60-70% of cases. On the other hand, the predator was almost always successful in catching prey when faced with a slow moving mill. Wood et al.'s (2007) study is important because it provides evidence that complex collective level phenomena can evolve between 'selfish' individuals without the need to invoke arguments based on kin selection or repeated interactions between individuals.